

Highlights

Low-cost real-time monitoring and automated control system for a bench-scale portable downdraft gasifier

Antonio Rodríguez Orta, Manuel Sánchez Raya, Roque Aguado Molina, Juan Antonio Gómez Galán, David Vera Candeas, Diego A. López García

- A low-cost system is developed with OTA updates and an intuitive interface.
- Various biomass types can be characterized with only a small amount of feedstock.
- The monitoring system is designed for easy operation and low maintenance.
- Target temperature is reached and stabilized within 20–25 minutes from room temperature.
- The system is stabilized through user adjustments within 10 minutes after steady state.

Low-cost real-time monitoring and automated control system for a bench-scale portable downdraft gasifier

Antonio Rodríguez Orta^a, Manuel Sánchez Raya^a, Roque Aguado Molina^b, Juan Antonio Gómez Galán^{a,*}, David Vera Candeas^b, Diego A. López García^a

^a*Departamento de Ingeniería Electrónica, Sistemas Informáticos y Automática, Escuela Técnica Superior de Ingeniería, Universidad de Huelva, Avda. de las Fuerzas Armadas s/n, 21007 Huelva, Spain*

^b*Departamento de Ingeniería Eléctrica, Escuela Politécnica Superior de Linares, Universidad de Jaén, Avda. de la Universidad s/n, 23700 Linares, Spain*

Abstract

This research work focuses on the development of a real-time monitoring and automated control system with remote access, as well as integrated data collection and storage, for a portable biomass gasification prototype to generate electricity from agricultural waste. The prototype consists of an air-blown downdraft fixed-bed gasifier and a producer gas conditioning unit, which operate together in a remotely controlled ensemble. The proposed system stands out for its compact size, transportability, and low-cost design, making it suitable for implementation in small agricultural facilities, especially in areas where conventional electrification is limited or non-existent. Two preliminary tests were conducted to evaluate the performance of the monitoring system. In the first test, the system achieved a target temperature of 600 °C in less than 20 minutes and maintained it within a variation range of ± 25 °C. After holding this temperature for an hour, the setpoint was raised to 800 °C, with the system achieving the new target in less than 10 minutes. In the second test, a setpoint of 800 °C was reached in 16 minutes, with an additional 3 minutes required for stabilization. Both tests, lasting approximately 4 hours each, consumed a total of 13.43 kg of biomass. The results demonstrate the system's ability to reach target temperatures in less than 25 minutes while maintaining stable temperature oscillations. The system's graphical interface enables intuitive, real-time, and remote monitoring and management of temperatures in several zones along the gasifier's height. Additionally, the interface allows manual or algorithmic control of the system's actuators, with the ability to modify the control algorithms through over-the-air updates.

Keywords: Biomass gasification, Producer gas, Process automation, Real-time system, Remote access, Low power consumption

*Corresponding author

Email addresses: antonio.rodriguez@diesia.uhu.es (Antonio Rodríguez Orta), msraya@diesia.uhu.es (Manuel Sánchez Raya), ramolina@ujaen.es (Roque Aguado Molina), jgalan@diesia.uhu.es (Juan Antonio Gómez Galán), dvera@ujaen.es (David Vera Candeas), diego.lopez@diesia.uhu.es (Diego A. López García)

1. Introduction

The agrifood industry is a significant contributor to global waste production, with large amounts of biomass generated during agricultural and food processing activities. If properly managed, agroindustrial waste holds significant potential to become a valuable resource for energy recovery, especially in remote locations with abundant biomass resources. One promising management approach is gasification, which allows agroindustrial waste to be used for decentralized renewable electricity generation [1]. This decentralized approach is particularly well-suited to the dispersed population and economic activities of rural regions, providing a practical alternative to reduce reliance on fossil fuel sources for electrification and increase energy security [2]. Moreover, gasification of agroindustrial waste reduces the need for open burning, thereby mitigating fire risks and decreasing greenhouse gas emissions. Local energy production can also boost economic development, create jobs, and improve living standards in rural communities. Furthermore, scalability and adaptability of gasification systems make them versatile, allowing them to be tailored to the varying energy needs and capacities of different rural areas.

Gasification is a thermochemical conversion process that involves subjecting a solid carbonaceous feedstock to partial oxidation with a gasifying agent, typically air, oxygen, steam, or combinations thereof [3, 4]. For small-scale gasification systems designed for electricity generation, air is usually the preferred option due to its economic advantages [5–7]. The air-blown gasification process allows organic carbon materials, such as agroindustrial biomass waste, to be converted into a lean fuel gas, known as producer gas, which is suitable for power generation [8, 9].

Gasifiers are broadly classified as fixed bed, fluidized bed, and entrained flow [3]. Fixed-bed gasifiers are in turn subcategorized into updraft, downdraft, and crossdraft types. Downdraft gasifiers are characterized by a parallel downward flow of both the solid feedstock and the gasifying agent. In this design, the gasifying agent (i.e., air) is introduced below the upper area and the producer gas is extracted through the lower part of the reactor. Downdraft gasifiers are the preferred option for small-scale distributed power generation due to their simple construction, reli-

27 able operation, short startup time (20–30 minutes), adaptability to various biomass feedstocks, and
28 high carbon conversion efficiency [3, 7, 10, 11]. As a result of these advantages, downdraft gasi-
29 fiers currently dominate the market, especially in power generation applications, accounting for
30 roughly three-fourths of all gasifiers marketed commercially [12]. Additionally, they produce less
31 tar because the oxidation zone immediately follows the pyrolysis zone, where these compounds
32 are formed [3]. This characteristic makes downdraft gasifiers particularly suitable for small-scale
33 electricity production with internal combustion engines (ICEs) [4], especially for applications re-
34 quiring up to 1 MW of thermal power [3]. However, the producer gas must be cooled before use
35 as a result of the high reactor outlet temperature [13]. Small-scale downdraft gasifiers provide the
36 added advantage of being containerizable for convenient transportation and can even be designed
37 as mobile power generation units [11]. These features make them particularly attractive for elec-
38 trifying isolated communities in rural areas [2, 14], as they can be operated in off-grid mode or
39 integrated into microgrids without the need for prior electrical infrastructure. As main drawbacks,
40 downdraft gasifiers generally exhibit lower thermal performance compared to other technologies
41 and may face challenges when processing biomass feedstocks with high ash and moisture content.
42 Downdraft gasifiers can be subclassified into two major design variants: throated (also known as
43 constricted) and throatless (also known as topless, open top, or open core). Constriction in the
44 combustion stage favors the thermal cracking of most of the tar by forcing all pyrolysis products
45 to pass through a narrow section, thus improving the quality of the producer gas [3, 15, 16].

46 The gasification process can be divided into four main stages: drying or dehydration, pyrolysis
47 or volatilization, combustion or oxidation, and gasification or reduction [3, 17, 18]. In fixed-bed
48 gasifiers, these reactions occur in specific areas, whereas, in fluidized-bed gasifiers, the reactions
49 can occur simultaneously throughout the reactor. However, during the actual operation, the four
50 reaction zones commonly overlap with no clear or discrete separation between them [17]. In the
51 drying stage, the solid fuel reaches temperatures up to 200–250 °C, losing most of its moisture
52 and reducing its content to around 5% [4, 19]. Pyrolysis follows, where biomass chemical bonds

53 break (thermolysis) at temperatures in the range of 150 to 700 °C, leading to pyrolytic products
54 (including both light and heavy hydrocarbons, the latter commonly known as tars) [3, 4, 18, 20].
55 Drying and volatilization occur simultaneously, producing gaseous, liquid, and solid fractions.
56 Non-condensable gases make up 70% to 90% by weight of the products [20]. In the combustion
57 zone, temperatures reach between 500 and 1500 °C due to exothermic oxidation of pyrolysis prod-
58 ucts in oxygen's presence [4, 21, 22]. Oxidation must occur with limited oxygen to avoid complete
59 fuel combustion [20]. Heat from combustion drives drying, pyrolysis, and gasification. Using air
60 as a gasifying agent introduces inert gases like nitrogen (N₂) and argon (Ar) into the product gas
61 [20]. Finally, in the gasification zone, hydrogen (H₂), carbon monoxide (CO), and methane (CH₄)
62 are formed through reduction reactions of oxidized carbonaceous solids with downstream gases.
63 This endothermic process occurs at temperatures in the range of 600 to 1100 °C [3, 20, 21]. As
64 temperature changes affect gas composition and tar concentration, strict control over the process
65 temperature is essential. Higher temperatures increase carbon conversion and reduce tar forma-
66 tion, but also lead to an increased risk of ash sintering and a decline in the calorific value of the
67 product gas [20].

68 Automation and control systems for biomass gasifiers have advanced significantly in recent
69 years. Early automation systems relied on basic functionalities such as temperature monitoring
70 or implementing proportional-integral-derivative (PID) controllers for specific process variables,
71 which proved inadequate for dynamic biomass conditions. Sagüés et al. [23] introduced a fuzzy
72 inference system (FIS) to control gasifiers, encoding expert knowledge into if-then rules. This
73 approach allowed the system to dynamically adjust process parameters like air flow and grate
74 frequency based on biomass type and moisture content, enhancing adaptability and process ef-
75 ficiency. Gandhi et al. [24] developed a fuzzy logic controller (FLC) for downdraft gasifiers,
76 utilizing a multi-input multi-output (MIMO) system to regulate temperature and CO/CO₂ ratio.
77 Their approach significantly improved stability and response time compared to conventional PID
78 controllers, demonstrating the effectiveness of FLC in handling the nonlinear dynamics of biomass

79 gasification. Gøbel et al. [25] advanced the field with a dynamic one-dimensional mathematical
80 model that incorporated conservation laws and reaction kinetics to optimize stationary perfor-
81 mance and identify efficient control strategies for handling load changes. Striūgas et al. [26]
82 further demonstrated practical advancements in automation by integrating staged air supplies,
83 moving grates, and pressure-based char discharge systems into multi-fuel downdraft gasifiers.
84 Their work highlighted the importance of controlling parameters such as bed pressure and tem-
85 perature to enable effective gasification of diverse biomass feedstocks. More recently, Daniel and
86 Gandhi [27] focused on improving PID controller performance for downdraft gasifiers by utiliz-
87 ing particle swarm optimization (PSO) and adaptive neuro-fuzzy inference system (ANFIS) tech-
88 niques. Their work demonstrated that PSO and ANFIS-based PID tuning outperformed traditional
89 Ziegler-Nichols methods in temperature control, providing better transient response and reduced
90 overshoot.

91 Despite the aforementioned improvements in the control and optimization of biomass gasi-
92 fiers, there are still numerous opportunities for further research. A remarkable gap in the relevant
93 scientific literature is the development of more intuitive, low-maintenance monitoring and auto-
94 mated control systems that are suitable for portable biomass gasifiers in remote locations. Many
95 existing systems tend to be complex and require skilled personnel for maintenance, which limits
96 their applicability in off-grid settings or underserved areas, where simplicity and reliability are
97 paramount. Moreover, attracting and retaining skilled operators for gasification systems remains
98 a significant challenge, particularly in rural and often remote areas [28]. Nonetheless, overcoming
99 these challenges could unlock the full potential of waste-to-energy solutions for the electrification
100 of isolated communities.

101 This paper presents an intuitive, low-maintenance monitoring system for a compact, portable
102 biomass gasifier intended for electric power generation in remote locations. Unlike traditional
103 systems, which are often complex and require skilled operators, the proposed system is specifically
104 designed for transportability, as well as ease of operation and maintenance. Additionally, the

105 compact control unit (housed in a $250 \times 250 \times 100$ mm waterproof enclosure) enhances portability,
106 enabling quick installation and flexible deployment in diverse environments. The proposed system
107 not only collects and stores operational data, but also provides real-time monitoring and remote
108 control capabilities, enabling adjustments to working temperatures to adapt to different biomass
109 types. These features make the system highly intuitive and user-friendly, addressing a gap in the
110 market for portable, easy-to-operate biomass gasifiers that can drive electrification in remote or
111 underserved areas.

112 **2. Methodology**

113 This section outlines the rationale behind the selected design, focusing on simplicity, cost-
114 effectiveness, and ease of use. The monitoring and automated control system features compact,
115 high-precision hardware utilizing low-cost commercial sensors and actuators. Additionally, an
116 intuitive graphical interface allows for straightforward remote management, enhancing both us-
117 ability and operational efficiency at physical and software levels.

118 *2.1. Biomass feedstock characterization and choice of gasifying agent*

119 Biomass gasification processes are inherently complex due to their multivariable, nonlinear
120 behavior, as well as the variability of biomass properties such as chemical composition, moisture
121 content, and particle size. In the experiments presented in this paper, olive pomace pellets were
122 used as feedstock, the physicochemical properties of which can be consulted in a previous work of
123 some of the authors [7]. Air was used as gasifying agent, due to its availability and low cost [6, 7].
124 As mentioned above, the resulting gaseous product from air-blown gasification is a lean fuel gas
125 with a high content of inert gases known as producer gas. Despite its relatively low calorific value,
126 it is still suitable for power generation using ICEs [9, 29].

127 2.2. Design of the biomass gasifier

128 Among the various available alternatives, a downdraft fixed-bed reactor was selected in this
129 study for the reasons outlined in Section 1. The height of the reactor is 1.4 m, making it easily
130 transportable. This reactor uses gravity as the driving force to move the fuel from the feed hop-
131 per (upper section) to the combustion zone (lower section), where the highest temperatures are
132 reached [3]. In this study, a downdraft reactor with a constriction in the combustion zone was
133 used. The inclusion of a constriction zone forces the products from pyrolysis to pass through a
134 narrow passage, where they undergo combustion in a process known as flaming pyrolysis, thereby
135 reducing the formation of tar [3, 18]. Furthermore, temperatures above 800 °C are reached, pro-
136 moting thermal cracking reactions, which significantly reduce the tar content in the producer gas
137 [30]. This reduction in tar content is critical, not only for improving the quality of the producer
138 gas but also for lowering the operation and maintenance costs, as tar deposits can lead to clogging
139 and damage to equipment.

140 The gasification process produces a lean fuel gas known as producer gas, which can be used to
141 power a generator set for electricity generation [9]. However, some impurities contained in the hot
142 producer gas, such as fly ash, tar, and moisture, can condense in the low-temperature sections and
143 adhere to the internal surfaces of the system, leading to severe fouling and corrosion issues [7]. For
144 this reason, the system incorporates gas conditioning and filtration elements downstream of the
145 reactor, ensuring continuous operation without frequent maintenance interruptions [4]. Another
146 design consideration is the elevated temperature at which the producer gas is generated, which
147 can be detrimental to the engine–generator set. To mitigate this issue, a heat exchanger is used to
148 reduce the outlet temperature. All these components, including the sensors, actuators, gas filtration
149 equipment, and adaptation components, are schematically illustrated in Fig. 1.

150 During operation, the gasification temperature is carefully adjusted by regulating the airflow
151 rate to strike a balance between the calorific value and yield of producer gas. These temperature
152 settings can be adjusted to adapt to variations in biomass composition, including moisture content,

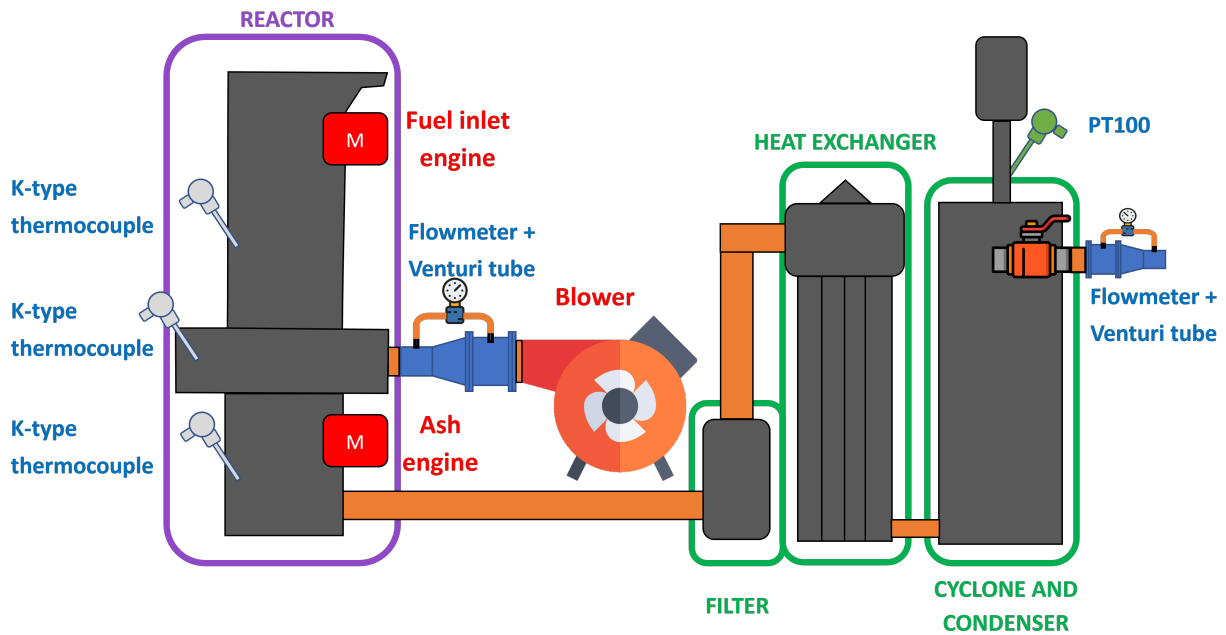


Figure 1: Overview of the prototype assembly, highlighting its main components.

153 ash content, and energy density, which significantly influence the performance of the gasification
 154 process. The system's programmable graphical interface allows users to manually or automatically
 155 modify the temperature set points and heating rates by manipulating the operation of the different
 156 motors, thereby providing real-time control over the gasification process.

157 Biomass decomposition under substoichiometric operating conditions generates a dense mist
 158 composed of water vapor and tar that adheres to the system walls and is carried downstream by
 159 the continuous flow of gas. The producer gas leaves the gasification reactor at around 400 °C [7],
 160 and contains particulates, condensates, tar, and water vapor [18]. This hot producer gas must be
 161 cooled and cleaned, ensuring it is virtually free from tar, water vapor, and particulates, and at near
 162 ambient temperature if it is to be utilized in an internal combustion engine [18]. In this study, a
 163 compact producer gas conditioning system is included to support extended operation with reduced
 164 maintenance (see Fig. 1). This system consists of a gas-air countercurrent-flow heat exchanger
 165 that lowers exhaust gas temperature from 400 °C to about 50 °C, suitable for the engine-generator
 166 set; a cyclone that redirects part of the inlet airflow to the heat exchanger outlet to avoid particle

167 buildup in the condenser; a condenser that traps contaminants at the bottom of a container to
168 prevent them from circulating through the piping; and an ash collection box with a removable
169 door for easy withdrawal of accumulated residues after several hours of operation.

170 *2.3. Operating procedure*

171 The first step is to load the reactor with the biomass feedstock and securely seal it against air
172 leakage [31]. Proper sealing is essential to maintain control over the reactor's internal conditions,
173 as the centrifugal blower is the sole component responsible for injecting a regulated amount of
174 air into the reactor. To ensure that the product gas is usable for power generation applications
175 and contains a minimal number of contaminants, the goal is to achieve a chemical decomposition
176 reaction of organic matter under substoichiometric conditions [3]. Gasification reactions occur at
177 elevated temperatures in an oxygen-lean atmosphere, which reflects the paramount importance of
178 an air-tight sealing [32–34].

179 After sealing against leakage, combustion must be initiated manually, a process that lasts for
180 approximately 20 min depending on the moisture content of the feedstock [7]. During this stage,
181 a blowtorch provides heat, and the blower injects as much air as possible, thereby promoting heat
182 distribution and the formation of the first layer of charred particles in the combustion chamber.
183 Once the process has become self-sustaining, the user can switch to automatic mode. In this
184 mode, the system automatically regulates the air intake to the reactor by adjusting the airflow
185 rate based on feedback from the temperature sensors integrated into the reactor. The aim of the
186 electronic system is to maintain operation within established temperature ranges, facilitating the
187 gravity-driven movement of the feedstock through the different sections of the reactor, while si-
188 multaneously eliminating ash deposits from the walls through vibrations generated by two motors
189 placed at the bottom of the reactor.

190 During the biomass gasification process, it is essential to maintain the temperature in the com-
191 bustion zone at around 800 °C to provide the required heat supply for the endothermic pyrolysis
192 and reduction reactions, as well as for minimizing tar production [5, 35, 36]. Tar is detrimental

193 to both the environment and the power generation unit, thereby reducing its lifespan [30]. The
194 producer gas from the reactor is at elevated temperatures and may contain impurities, necessitat-
195 ing pretreatment before it can be used in an engine. Filtration removes impurities such as dust,
196 tar, and moisture, which may clog the intake manifold of the engine and increase maintenance
197 requirements. The heat exchanger reduces the gas temperature from approximately 400 °C at the
198 reactor outlet to around 50 °C, making it suitable for engine operation. After the conditioning
199 stage, the system is equipped with a T-valve that allows the producer gas to be routed either to the
200 flare stack or to the generator set. An effective approach to determine whether the producer gas
201 has an adequate calorific value is to ignite it. A blue flame indicates the gas is appropriate for use
202 as fuel [7], thereby avoiding the need for an expensive gas analyzer.

203 *2.4. Hardware design*

204 Temperature and airflow sensors were strategically placed to evaluate the performance of the
205 prototype and determine whether they satisfy the design specifications. These sensors provide
206 real-time data on the state of the system, enabling the implementation of necessary actions to sta-
207 bilize the pyrolysis reaction. The key parameter for maintaining this reaction is the combustion
208 temperature. The reactor, in conjunction with the control unit, must sustain the temperature at
209 approximately 800 °C, with a narrow allowable range (± 25 °C). Temperature stability depends
210 on the volume of air introduced as an oxidizer. The control unit adjusts the control signal using
211 pulse width modulation (PWM) of the blower based on the data provided by the temperature sen-
212 sors. Unlike all-or-nothing control, where the system operates only in states of maximum or no
213 power, PWM allows continuous adjustment of energy without incurring the significant thermal
214 losses associated with linear regulation. This is because the switching devices used in PWM op-
215 erate in saturation or cut-off modes, minimizing power dissipation [37]. In addition, PWM offers
216 a more efficient response in terms of stability and speed control, reducing sudden fluctuations in
217 flow pressure and allowing better adaptation to the dynamic conditions of the system. This fea-
218 ture is essential in applications that require precise flow regulation without introducing additional

219 disturbances to the flow measurement [38].

220 2.4.1. Sensors

221 Industrial-grade sensors were selected to characterize the biomass gasifier prototype. These
222 sensors feature specially designed and sealed enclosures to operate in environments with contam-
223 inants, such as dust and splashes. They also incorporate 4–20-mA industrial standard transducers,
224 which are known for their immunity to the electromagnetic noise generated by motors [39, 40].
225 In the prototype, potential sources of electromagnetic noise that could negatively impact the in-
226 strumentation include the motors responsible for dislodging ash from the reactor walls, facilitating
227 fuel descent into the combustion chamber, as well as the blower motor.

228 K-type thermocouples, with a temperature range of 0–1200 °C, were placed at different sec-
229 tions along the vertical axis of the reactor [41]. Additionally, a PT100 sensor, with a temperature
230 range of 0–100 °C, was chosen to monitor the performance of the heat exchanger, ensuring that
231 the temperature is reduced to approximately 50 °C. The PT100 sensor provides a higher resolution
232 within its operating range than the thermocouples, justifying the change in sensor type. Differen-
233 tial pressure sensors coupled with properly sized Venturi tubes were used to measure the airflow
234 at the inlet and outlet of the prototype. This setup generates a pressure variation (ΔP) proportional
235 to the airflow rate (Q), as indicated in Eq. (1).

$$\Delta P = P_1 - P_2 = \frac{Q^2 \rho (A_1^2 - A_2^2)}{2 A_1^2 A_2^2} \quad (1)$$

236 where A denotes the internal cross-sectional area of the tube and ρ represents the gas density.
237 Subscripts 1 and 2 correspond to the converging conical section and the throat section of the
238 Venturi flow meter, respectively.

239 This combination is preferred in industrial settings for fluids prone to contamination, where
240 other measurement devices such as rotameters are inoperative.

241 2.4.2. *Actuators*

242 To ensure efficient gasifier operation, several physical components were integrated to enhance
243 system performance and control. The blower adjusts combustion temperature by regulating the
244 airflow rate injected into the reactor, increasing the oxidizing agent and allowing higher combus-
245 tion temperatures. Agitator motors prevent the buildup of plant-based fuel on the reactor walls,
246 promoting its movement to the combustion zone by gravity and avoiding ash accumulation. Ad-
247 ditionally, a T-valve connected to a chimney redirects the producer gas either for incineration in a
248 flare stack or to the engine intake manifold based on a test of the flame's color. The flame should
249 turn blue to confirm that the gas is sufficiently clean and tar-free. This configuration enables real-
250 time verification that the target reaction temperature, approximately 800 °C, has been reached.

251 2.4.3. *Wireless control system*

252 Data collection was performed wirelessly, allowing the operators to interact with the system
253 in real time, even in manual mode, without the need to open the sealed control unit enclosure.
254 Despite the wireless nature of data transmission, it is crucial to maintain secure communication
255 between the system and the computer without data loss. A web interface was developed to help
256 visualize the data and control the various system components. Through this interface, users can
257 access historical measurement records, calibrate sensors, adjust control parameters, and set target
258 temperatures.

259 The system was designed to monitor and control the prototype autonomously, although man-
260 ual ignition is required during the initial phase. All the measurements and actuator inputs were
261 stored locally on a microSD card, complete with timestamps. With each new data collection, these
262 measurements were updated and displayed on the user's graphical web interface, allowing for the
263 detection of irregularities and monitoring of the system's overall performance.

264 The control system comprised a control unit, real-time clock (RTC), microSD card slot, con-
265 nectors for the 4–20-mA sensors, power supply system, and power-consuming elements. These

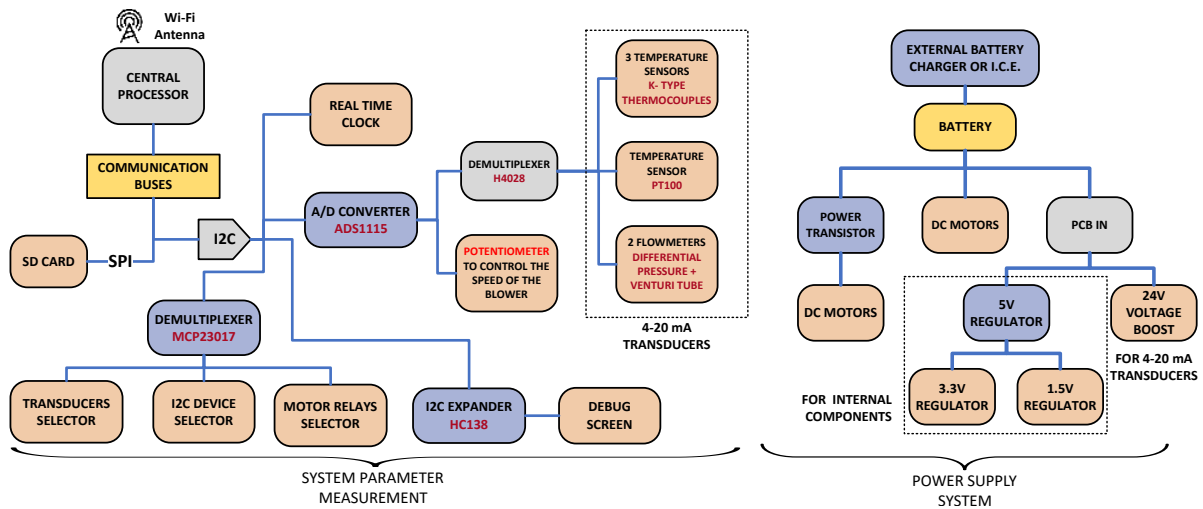


Figure 2: Schematic diagram of the main hardware elements.

266 elements included relays for motor actuation (without regulation) and a power stage for precise
 267 control of the blower motor. A schematic diagram of the control system is illustrated in Fig. 2.

268 The principal component of the control unit is an ESP32 microcontroller (Espressif Systems).
 269 This system-on-chip integrates two ultralow-power processors, offering robust computational ca-
 270 pabilities while minimizing energy consumption. ESP32 can implement multiple communication
 271 protocols, including SPI and I2C, which are essential for interfacing various sensors and actuators
 272 within a system [42, 43]. Furthermore, ESP32 supports wireless connectivity in the 2.4-GHz band,
 273 incorporating both Bluetooth and Wi-Fi transceivers, which facilitate seamless data transmission
 274 and remote monitoring.

275 The printed circuit board (PCB) is complemented by additional key components, as shown in
 276 Fig. 3. These elements enhance the functionality and reliability of the control unit, thereby en-
 277 suring the efficient operation of the gasification system. The PCB integrates power management
 278 circuits to stabilize the supply voltage, signal conditioning modules for accurate sensor data acqui-
 279 sition, and communication interfaces to ensure reliable data exchange between the microcontroller
 280 and the peripheral devices.

281 Incorporating an ESP32 microcontroller into the control unit design provides a versatile plat-

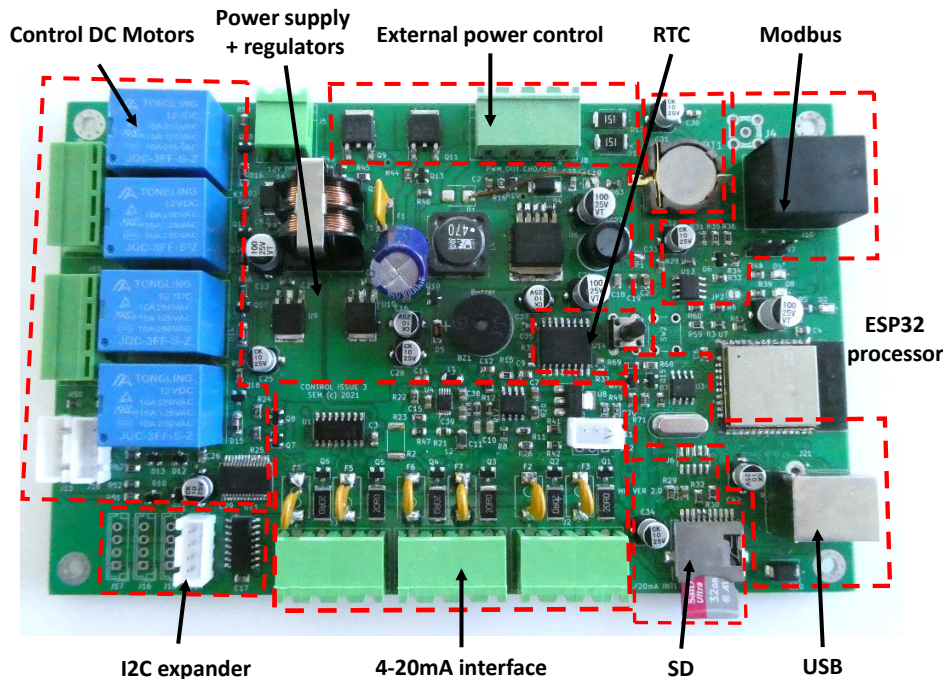


Figure 3: Prototype control unit hardware.

282 form capable of managing complex control tasks and real-time data processing. Its wireless com-
 283 munication capabilities also enable remote monitoring and control, which are critical for optimiz-
 284 ing the performance and safety of the gasification process. The integration of these features into
 285 a compact, energy-efficient design underscores the suitability of ESP32 for industrial applications
 286 such as biomass gasification.

287 2.4.4. Measurements of temperature and gas flow rate

288 To measure the gas temperature and flow, the instrumentation system employs industrial sen-
 289 sors that incorporate standard 4–20-mA transceivers. These transceivers require a supply voltage
 290 of 24 V, which is provided by a voltage booster integrated into the system. Sensors consume
 291 minimal energy; therefore, a high current supply is unnecessary.

292 Temperature was measured inside the reactor using three K-type thermocouples located at dif-
 293 ferent zones such as drying–pyrolysis, oxidation, and reduction [26, 27]. A PT100 sensor was
 294 used at the gas outlet of the system to ensure that the heat exchanger operated correctly and that

295 the producer gas could be safely introduced into the ICE without causing damage. Differential
296 pressure sensors coupled with Venturi tubes were used to measure the inlet airflow and the syn-
297 thesis gas flow at the outlet. The resulting pressure difference ($\Delta P = P_1 - P_2$) allows for direct
298 calculation of the fluid flow rate (Q), as follows:

$$Q = A_1 A_2 \sqrt{\frac{2(P_1 - P_2)}{\rho(A_1^2 - A_2^2)}} \quad (2)$$

299 To optimize the design and reduce the size of the measurement hardware, the instrumentation
300 system employed a single ADS1115 analogue-to-digital (A/D) converter, necessitating the use of
301 a demultiplexer for all 4–20-mA analogue inputs.

302 The transceivers are not designed for immediate operation; they require a stabilization time
303 of approximately 6 seconds after being powered, totaling approximately 36 seconds for the six
304 sensors. To bypass this delay, a resistor connected to the negative pole of each transceiver was
305 used to continuously power it. When a data sample is required, the transistor redirects the current
306 from each input to the A/D converter without disrupting operation. This approach enables the
307 instant measurement of all parameters.

308 To verify the behavior and linearity of the system in response to changes in the flow rate and
309 temperature, each sensor was calibrated in the laboratory. This process included setting up differ-
310 ent valves that redirected the airflow towards either the reactor or the exhaust. The reduction in the
311 cross section of the air hoses was considered in the calculations because it imposes a limitation on
312 the maximum flow rate that can be supplied by the blower.

313 For temperature calibration, a calibrated PT100 sensor and a type-K thermocouple (RS Ami-
314 data) were used. The differential pressure gauges were calibrated with a high-power blower, ex-
315 ceeding the power of the blower eventually installed in the prototype, along with a pressure meter
316 capable of measuring up to 200 slm (12 m³/h).

317 2.4.5. *Power supply system*

318 The system is powered by a gel battery designed for photovoltaic systems, which provides a
319 voltage of 12 V and can supply a high current. Once electricity is generated, the battery can be
320 charged using a photovoltaic panel or by the system itself. During the experiments, the battery
321 was charged in the laboratory using a mobile battery charger.

322 The system operates at five different voltages on the printed circuit board:

- 323 • 12 V: Supplied by the battery, from which the remaining voltages in the system arise.
324 Through a series of protective fuses, it also provides a high current to components, such
325 as the agitator motors responsible for ash removal and the movement of solid fuel inside the
326 reactor, as well as feeds the transistor that regulates the blower.
- 327 • 24 V: Generated by an embedded converter (XL6009) capable of supplying up to 1A, this
328 voltage powers the 4–20-mA transceivers. Each device is equipped with a PolyFuse (PTC-
329 based resettable fuse) thermistor to prevent control unit issues in the event of an external
330 short circuit, opening the circuit until the issue is resolved.
- 331 • 5, 3, and 1.5 V: These voltages are provided by AMS1117-XX linear low-dropout regulators
332 and are used to power various integrated circuits within the system.

333 2.4.6. *Power consuming elements*

334 Both the motors that vibrate the reactor and the blower that drives air for combustion are pow-
335 ered by a 12-V battery. The motors operate using a simple on/off control mechanism implemented
336 through relays. By contrast, the blower utilizes a PID control system that modulates the power
337 supply using PWM and an external power transistor.

338 2.5. *Firmware and software*

339 This section describes the software and firmware that make up the control system, includ-
340 ing task management, interaction with the web interface, and flexible programming for process
341 automation and real-time monitoring.

342 2.5.1. Firmware

343 To provide robustness against failures during operation and allow the parallelization of differ-
344 ent tasks to be performed by the control unit, the FreeRTOS operating system was implemented.
345 RTOS allows the programmer to define tasks and set execution priorities, thereby ensuring that the
346 system works as planned. To prevent data loss, data are stored locally on a microSD card, which
347 also supports remote access.

348 If the system must stop immediately, the monitoring will continue without corrupting the data
349 as long as the power is not cut or the user stops it; therefore, turning off the system and removing
350 the microSD card could allow access to the information provided by the different sensors and the
351 system to be able to locate and correct malfunctions.

352 The process of data acquisition and system control is composed of seven main tasks, which are
353 illustrated in the simplified workflow diagram in Fig. 4. These tasks include Wi-Fi TCP/IP com-
354 munication, firmware update, web server request processor, web socket data interchange, sensor
355 data capture, automatic mode interpreter, and the PID power control loop.

356 Upon startup, all tasks are initialized and stored in static memory, remaining in a standby
357 state until an event allows them to continue. Initially, the system attempts to establish a wireless
358 connection with a known Wi-Fi network. If no connection is achieved after several attempts,
359 the system creates a new network (access point mode) such that the user can access the control
360 and monitoring interface provided by the internal web server. Web server pages are stored in the
361 internal memory of the microcontroller; therefore, if the SD card is removed or damaged, the
362 server will continue to work. In addition, the web server allows for the review and configuration
363 of the sensor calibration values.

364 By default, the system starts in manual mode, allowing the user to control the motors and inlet
365 airflow through a remote web user interface. This manual control allows for ignition and reactor
366 initiation. The user can also control the data acquisition. Once the gasification process inside the
367 reactor is started, the system can be switched to automatic mode. In this mode, the control unit

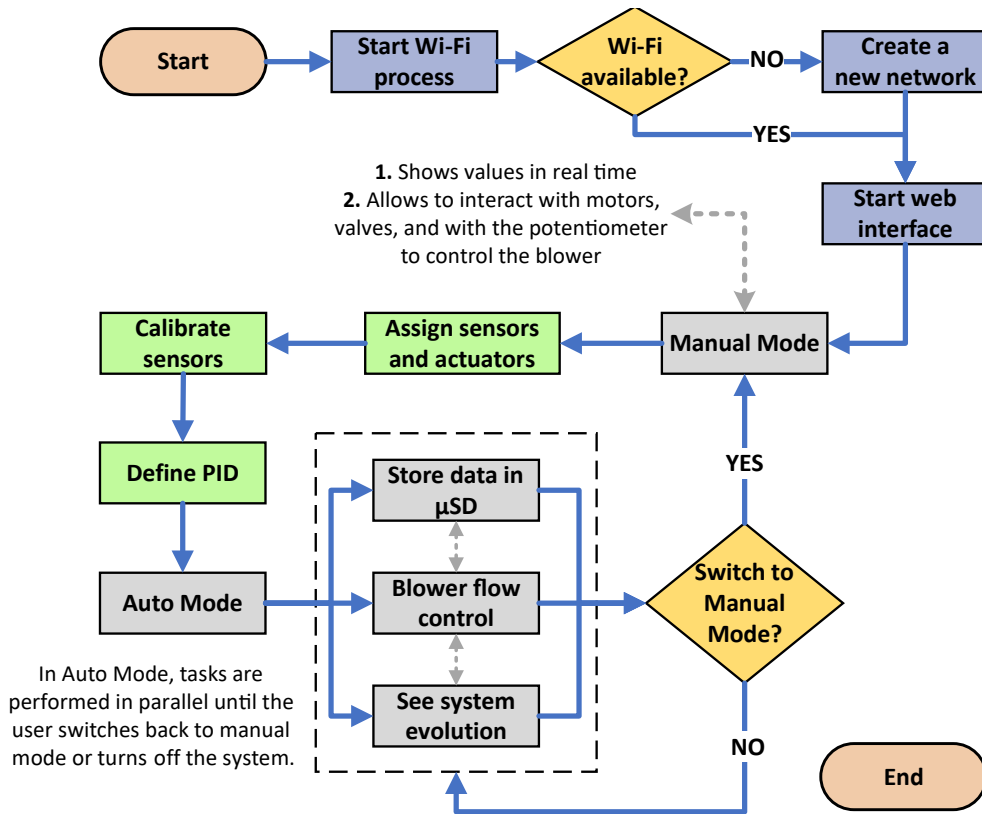


Figure 4: Schematic workflow diagram of the firmware operation.

368 is responsible for maintaining the desired temperature by adjusting the inlet airflow to regulate
 369 combustion.

370 2.5.2. Software

371 The control unit utilizes a programming language that allows users to define the operating
 372 time intervals for each motor. System behavior is configured using a sequential instruction-based
 373 language, such as BASIC. Users can start, stop, or modify a program interactively and remotely
 374 via a command-line interface. This customizable approach offers significant system flexibility, en-
 375 abling future automation of processes such as system startup or generator control by incorporating
 376 the necessary instructions.

377 By default, the system operates in automatic mode, requiring no user interaction. In the event
 378 of communication loss, the system continues functioning independently. The graphical user inter-

379 face provides real-time visualization of variable trends, temperature setpoint adjustment, sensor
380 calibration, OTA updates, and remote data retrieval from the memory card. In manual mode, users
381 can also adjust blower power as desired.

382 Due to the system's high thermal inertia, constant interaction with the blower's flow control
383 is unnecessary. To save resources, measurements can be recorded every 30 seconds. However, to
384 obtain more precise monitoring curves, measurements should be updated every second.

385 **3. Results and discussion**

386 To validate the system's functionality and its responsiveness to user demands, two field tests
387 were conducted. The aim of both tests was to investigate the temperature behavior inside the
388 gasifier, as well as the ability of the automated control system to maintain the target temperature.
389 The system was fully loaded to its maximum capacity with 26.62 kg of olive pomace pellets and
390 then started from ambient conditions (approx. 25 °C).

391 The first test aimed to evaluate the system's response to changes in predefined working con-
392 ditions. According to the scientific literature [27], airflow rate and biomass type are the most
393 important factors affecting the temperature in biomass gasifiers. Temperature control is relatively
394 straightforward and depends directly upon the supplied amount of air [26]. Initially, a temperature
395 setpoint of 600 °C was established. After the system stabilized at this temperature, the setpoint
396 was raised to 800 °C. The transition to the higher temperature took approximately 10 minutes,
397 during which the system maintained stability at the new temperature.

398 The second test focused on achieving 800 °C, starting again from ambient conditions. This
399 temperature aligns with the typical operating conditions for temperature control in downdraft
400 gasifiers, as documented in the scientific literature [26, 27]. Once both tests were completed,
401 the system was opened for cleaning, and the remaining charred feedstock was weighed. Overall,
402 13.43 kg of biomass feedstock was consumed during the tests. The experimental setup used for
403 the field tests is shown in Fig. 5.



Figure 5: Images of the reactor prototype, including a close-up view of the control system.

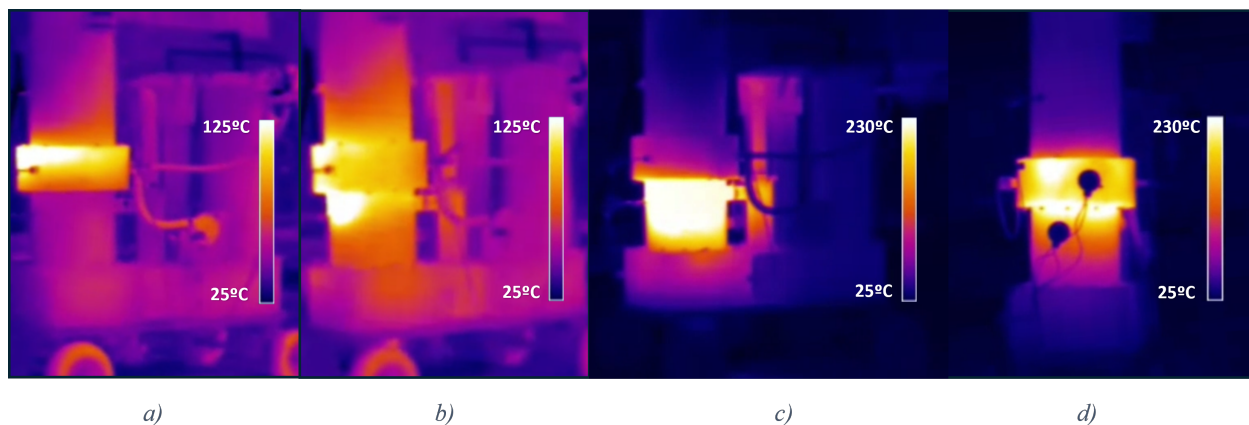


Figure 6: *a)* Combustion zone during startup *b)* Temperature distribution in the reactor within approximately 30 minutes from startup *c)* Temperature distribution in the reactor around one hour after startup *d)* Temperature distribution in the reactor during steady-state operation showing the placement of thermocouples.

404 During the first test, a thermal imaging camera (SATIR D600, Ireland) was used to monitor
 405 the system's performance throughout the transitional phase. Fig. 6 shows four thermal images
 406 captured at different intervals, illustrating the temperature distribution across the reactor's external
 407 surface. The process began with heat generation in the combustion zone, which then propagated to
 408 the adjacent pyrolysis and gasification zones. The surface temperature peaked at 125 °C during the
 409 external heat supply via a blowtorch and stabilized around 230 °C during steady-state operation.

410 The significant temperature gradient observed between the interior (800 °C) and the exterior (230
411 °C) of the gasification reactor reflects the system's high insulation efficiency.

412 *3.1. System performance during the first startup phase*

413 The initial startup was conducted on May 27, 2024, to evaluate whether the control system
414 could maintain a stable temperature in the reactor's central zone. During this test, the temperature
415 was initially set at approximately 600°C, with a tolerance of $\pm 25^\circ\text{C}$, before being raised to a final
416 target of 800°C. The behavior observed in this test is illustrated in Fig. 7 a), where significant
417 variations in temperature readings are observed across different zones of the reactor along with
418 the inlet air and outlet producer gas flow rates. Specifically, temperatures in the lower, middle,
419 and upper zones varied considerably, considering that these sensors are only 30 cm apart. This
420 variation can be attributed to the natural thermal gradients that occur in biomass gasification reac-
421 tors, where the combustion zone is typically much hotter than the reduction and pyrolysis zones.
422 The temperature distribution across the reactor is influenced by the composition and downward
423 movement of the fuel, the airflow rate, and the heat transfer processes. The producer gas outlet
424 temperature remained consistently stable at approximately 40 °C due to the effective operation of
425 the heat exchanger, ensuring its suitability for use in internal combustion engines [7].

426 Flow measurement exhibits significant noise due to the inherent nature of the flow sensing
427 system, which is subject to constant small pressure fluctuations. These variations arise from the
428 blower blade position, which may either have just passed or be actively pushing air at each mea-
429 surement point. Fig. 7 b) illustrates the behavior of the control signal, which regulates the power
430 supplied to the blower, compared to the instantaneous flow rates measured with flow meters.

431 In Fig. 7 a), it can be observed that after seven and a half minutes, a temperature of around 400
432 °C in the reduction zone at the reactor's lower section was reached, at which point the automatic
433 mode could be activated. In automatic mode, the system first aims to reach the target temperature
434 by increasing air intake to promote combustion, as reflected by the initial sharp increase in the
435 airflow rate, as can be observed in Fig. 7 a) and b). Once the target temperature is reached,

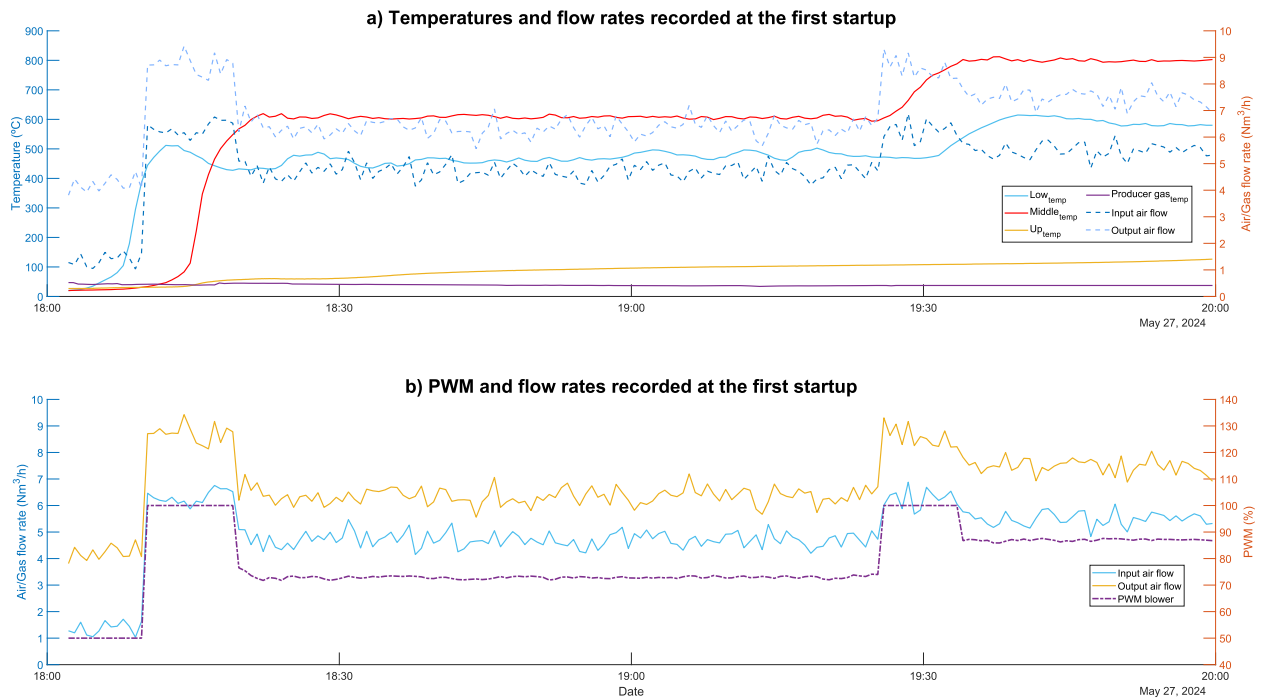


Figure 7: Temperatures, air and producer gas flow rates, and PWM recorded during the first startup.

436 the system regulates the incoming airflow to maintain the setpoint temperature until deactivation,
 437 shutdown, or the establishment of a new operating temperature. As evidenced, the control strategy,
 438 based on PWM, allows for precise adjustment of the blower power, enabling fine-tuned control
 439 over the reactor temperature. Any temperature deviations are addressed promptly through this
 440 feedback mechanism, which adjusts the blower's operation. The rapid response of the system
 441 ensures that the desired temperature is achieved within minutes, maintaining the stability and
 442 efficiency of the gasification process.

443 3.2. System performance during the second startup phase

444 The second startup aimed to replicate a more realistic operating condition by directly targeting
 445 a set-point temperature of 800 ± 25 °C in the combustion zone. Automatic mode was activated
 446 after an 8-minute startup phase. The system reached the target temperature within 16 minutes
 447 and stabilized it in approximately 3 additional minutes, maintaining a uniform temperature for the
 448 entire two-hour test duration. The temperature behavior throughout the process is presented in Fig.

449 8 a), displaying the temperatures in the lower, middle, and upper zones of the reactor, along with
 450 the producer gas temperature at the reactor outlet. The blower-induced airflow and the producer
 451 gas flow rate at the outlet are also shown in Fig. 8 a).

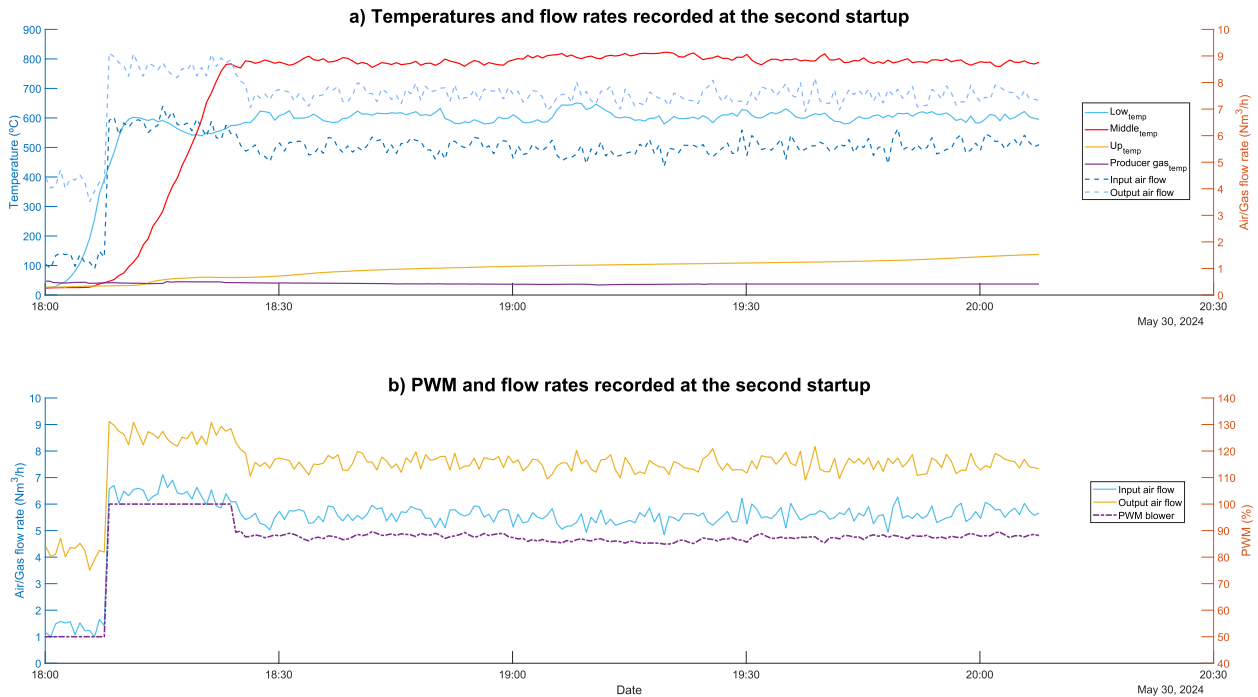


Figure 8: Temperatures, air and producer gas flow rates, and PWM recorded during the second startup.

452 Similar to the first test, Fig. 8 b) reveals some instability in airflow measurements caused by
 453 minor pressure fluctuations inherent to the blower's operation, which did not significantly affect
 454 system performance. Despite this slight instability induced by the blower, the control signal anal-
 455 ysis in Fig. 8 b) indicates minimal variation between input and output temperatures and flow rates,
 456 demonstrating an overall stable and reliable system performance.

457 **4. Conclusions and future outlook**

458 The biomass gasification technology presents substantial potential for the utilization of agri-
459 cultural waste. As demonstrated in this study, monitoring and automated control systems facilitate
460 the widespread use of portable gasification systems to support electrification in off-grid areas, such
461 as remote or isolated regions (including rural areas), due to their low cost, compact size, ease of
462 handling and maintenance, and adaptability to various biomass sources. Moreover, these versatile
463 systems constitute a valuable research tool for testing the gasification performance with diverse
464 biomass types, thus facilitating the determination of key parameters in the design of larger-scale
465 gasification plants.

466 The ESP32-based control system with FreeRTOS not only efficiently manages the gasifica-
467 tion process, but also possesses computational capacity beyond immediate needs. This means that
468 while the system awaits key events, its processor has ample resources to handle additional tasks
469 without compromising performance. Thanks to these features, it is possible to integrate additional
470 sensors (such as two 4–20 mA sensors), expand communication with I2C devices, and even coor-
471 dinate various gasifiers simultaneously via wireless connectivity or the Modbus protocol, which is
472 widely used in industry. Beyond energy management optimization, this capability also enables the
473 implementation of a parallel redundant system, ensuring continuous operation in case of failures
474 or maintenance. All of this can be achieved without major modifications to the current design,
475 reinforcing the flexibility and scalability of the solution. Furthermore, remote access through an
476 intuitive mobile interface not only simplifies system operation but also bridges the gap between
477 technology and its users.

478 Even though the current system represents a significant advancement in portable biomass gasi-
479 fication, there are several opportunities for future development. One key area for improvement
480 is the integration of modern optimization techniques, such as model predictive control or particle
481 swarm optimization, which could enhance the performance of the system by dynamically adjusting
482 parameters like air flow rate and temperature setpoints. Implementing such optimization strategies

483 could further improve system efficiency, adaptability to different biomass types, and overall stabil-
484 ity under varying operational conditions.

485 Future studies could focus on exploring the use of different biomass types to assess their im-
486 pact on system performance. Additionally, efforts could be made to improve the startup process,
487 making it fully automated, as well as to develop an automatic biomass feeding system. Moreover,
488 exploring the use and control of the engine-generator set through the same control board would
489 simplify the system architecture. Another promising direction for improvement involves expand-
490 ing the system's capabilities by integrating additional sensors, optimizing communication proto-
491 cols for large-scale deployments, and further enhancing the user experience through even more
492 intuitive control interfaces. These advancements would facilitate the wider adoption of biomass
493 gasification systems for sustainable energy production in remote and off-grid regions.

494 **Nomenclature**

495 **Abbreviations**

496 A/D Analog to digital

497 ANFIS Adaptive neuro-fuzzy inference sys-
498 tem

499 FIS Fuzzy inference system

500 FLC Fuzzy logic controller

501 I2C Inter-integrated circuit

502 ICE Internal combustion engine

503 MIMO Multi-input multi-output

504 OTA Over the air

505 PCB Printed circuit board

506 PID Proportional integral derivative

507 PSO Particle swarm optimization

508 PTC Positive temperature coefficient

509 PWM Pulse width modulation

510 RTC Real-time clock

511 RTOS Real-time operating system

512 SPI Serial peripheral interface

513 **Credit authorship contribution statement**

514 **A. Rodríguez Orta:** Conceptualization, Data curation, Formal analysis, Investigation, Method-
515 ology, Software, Validation, Visualization, Writing - Original Draft, Writing - Review & Editing.

516 **M. Sánchez Raya:** Conceptualization, Formal analysis, Investigation, Methodology, Software,

517 Validation. **R. Aguado Molina:** Conceptualization, Formal analysis, Investigation, Methodology,
518 Validation, Visualization, Writing - Original Draft, Writing - Review & Editing. **J.A. Gómez**
519 **Galán:** Conceptualization, Funding acquisition, Resources, Supervision, Validation, Writing -
520 Review & Editing. **D. Vera Candeas:** Conceptualization, Funding acquisition, Project admin-
521 istration, Resources, Supervision, Validation, Writing - Review & Editing. **D.A. López García:**
522 Conceptualization, Formal analysis, Investigation, Validation.

523 **Declaration of competing interest**

524 The authors declare that they have no known competing financial interests or personal rela-
525 tionships that could have appeared to influence the work reported in this paper.

526 **Funding**

527 This research work was supported by the project entitled “Renewable energies for Africa: Ef-
528 fective valorisation of agri-food wastes (REFFECT AFRICA)”, which has received funding from
529 the *European Union’s Horizon 2020 Research and Innovation Programme* under the following
530 Grant Agreement ID number: [101036900](https://doi.org/10.101036900).

531 **References**

- 532 [1] R. Aguado, D. Vera, D. A. López-García, J. P. Torreglosa, F. Jurado, Techno-economic assessment of a gasi-
533 fication plant for distributed cogeneration in the agrifood sector, *Appl. Sci.* 11 (2) (2021). [doi:10.3390/](https://doi.org/10.3390/app11020660)
534 [app11020660](https://doi.org/10.3390/app11020660).
- 535 [2] R. Aguado, D. Sánchez-Lozano, A. Escámez, D. Vera, F. Jurado Melguizo, 2 - gasification for electrification of
536 rural areas, in: M. Tostado-Véliz, A. Rezaee Jordehi, S. A. Mansouri, A. Ramos Galán, F. J. Melguizo (Eds.),
537 *Towards Future Smart Power Systems with High Penetration of Renewables*, Academic Press, 2025, pp. 23–52.
538 [doi:10.1016/B978-0-443-29871-4.00002-6](https://doi.org/10.1016/B978-0-443-29871-4.00002-6).
- 539 [3] P. Basu, *Biomass gasification, pyrolysis and torrefaction: Practical design and theory*, Elsevier, 2018. [doi:](https://doi.org/10.1016/C2016-0-04056-1)
540 [10.1016/C2016-0-04056-1](https://doi.org/10.1016/C2016-0-04056-1).

- 541 [4] R. Raj, D. Kumar Singh, J. Tirkey, Co-gasification of Low-grade coal with *Madhuca longifolia* (Mahua) biomass
542 and dual-fuelled mode engine performance: Effect of biomass blend and engine operating condition, *Energy*
543 *Convers. Manag.* 269 (2022) 116150. doi:10.1016/j.enconman.2022.116150.
- 544 [5] D. Vera, F. Jurado, K. D. Panopoulos, P. Grammelis, Modelling of biomass gasifier and microturbine for the
545 olive oil industry, *Int. J. Energy Res.* 36 (3) (2012) 355–367. doi:10.1002/er.1802.
- 546 [6] D. Vera, F. Jurado, N. K. Margaritis, P. Grammelis, Experimental and economic study of a gasification plant
547 fuelled with olive industry wastes, *Energy Sustain. Dev.* 23 (2014) 247–257. doi:10.1016/j.esd.2014.09.
548 011.
- 549 [7] R. Aguado, A. Escámez, F. Jurado, D. Vera, Experimental assessment of a pilot-scale gasification plant fueled
550 with olive pomace pellets for combined power, heat and biochar production, *Fuel* 344 (2023) 128127. doi:
551 10.1016/j.fuel.2023.128127.
- 552 [8] C. Higman, M. V. der Burgt, *Gasification*, *Gasification* (2008) 1–435doi:10.1016/B978-0-7506-8528-3.
553 X0001-6.
- 554 [9] F. Y. Hagos, A. R. A. Aziz, S. A. Sulaiman, Trends of syngas as a fuel in internal combustion engines, *Adv.*
555 *Mech. Eng.* 6 (2014) 401587. doi:10.1155/2014/401587.
- 556 [10] A. V. Bridgwater, The technical and economic feasibility of biomass gasification for power generation, *Fuel* 74
557 (1995) 631–653. doi:10.1016/0016-2361(95)00001-L.
- 558 [11] P. R. Bhoi, R. L. Huhnke, A. Kumar, S. Thapa, N. Indrawan, Scale-up of a downdraft gasifier system for
559 commercial scale mobile power generation, *Renew. Energy* 118 (2018) 25–33. doi:10.1016/j.renene.
560 2017.11.002.
- 561 [12] A. Kushwah, T. Reina, M. Short, Modelling approaches for biomass gasifiers: A comprehensive overview, *Sci.*
562 *Total Environ.* 834 (2022) 155243. doi:10.1016/j.scitotenv.2022.155243.
- 563 [13] M. Asadullah, Barriers of commercial power generation using biomass gasification gas: A review, *Renew. Sust.*
564 *Energ. Rev.* 29 (2014) 201–215. doi:10.1016/j.rser.2013.08.074.
- 565 [14] P. Sharma, B. Gupta, M. Pandey, K. S. Bisen, P. Baredar, Downdraft biomass gasification: A review on concepts,
566 designs analysis, modelling and recent advances, *Materials Today: Proceedings* 46 (2021) 5333–5341. doi:
567 10.1016/j.matpr.2020.08.789.
- 568 [15] E. Shayan, V. Zare, I. Mirzaee, Hydrogen production from biomass gasification; a theoretical comparison of
569 using different gasification agents, *Energy Convers. Manag.* 159 (2018) 30–41. doi:10.1016/j.enconman.
570 2017.12.096.
- 571 [16] S. Heidenreich, M. Müller, P. U. Foscolo, Advanced biomass gasification: New concepts for efficiency increase

- 572 and product flexibility, *Advanced Biomass Gasification: New Concepts for Efficiency Increase and Product*
573 *Flexibility* (2016) 1–134 [doi:10.1016/C2015-0-01777-4](https://doi.org/10.1016/C2015-0-01777-4).
- 574 [17] D. Thimsen, R. Maurer, A. Pooler, D. Pui, B. Liu, D. Kittelson, Fixed-bed gasification research using US coals.
575 Volume 14. Gasification of Kemmerer subbituminous coal, Bureau of Mines United States Department of the
576 Interior, 1985. [doi:10.2172/5868732](https://doi.org/10.2172/5868732).
- 577 [18] M. Dogru, Experimental results of olive pits gasification in a fixed bed downdraft gasifier system, *Int. J. Green*
578 *Energy* 10 (4) (2013) 348–361. [doi:10.1080/15435075.2012.655351](https://doi.org/10.1080/15435075.2012.655351).
- 579 [19] T. K. Patra, P. N. Sheth, Biomass gasification models for downdraft gasifier: A state-of-the-art review, *Renew.*
580 *Sust. Energ. Rev.* 50 (2015) 583–593. [doi:10.1016/j.rser.2015.05.012](https://doi.org/10.1016/j.rser.2015.05.012).
- 581 [20] A. Molino, S. Chianese, D. Musmarra, Biomass gasification technology: The state of the art overview, *J. Energy*
582 *Chemistry* 25 (2016) 10–25. [doi:10.1016/j.jechem.2015.11.005](https://doi.org/10.1016/j.jechem.2015.11.005).
- 583 [21] D. Baruah, D. C. Baruah, Modeling of biomass gasification: A review, *Renew. Sust. Energ. Rev.* 39 (2014)
584 806–815. [doi:10.1016/j.rser.2014.07.129](https://doi.org/10.1016/j.rser.2014.07.129).
- 585 [22] S. K. Sansaniwal, K. Pal, M. A. Rosen, S. K. Tyagi, Recent advances in the development of biomass gasification
586 technology: A comprehensive review, *Renew. Sust. Energ. Rev.* 72 (2017) 363–384. [doi:10.1016/j.rser.](https://doi.org/10.1016/j.rser.2017.01.038)
587 [2017.01.038](https://doi.org/10.1016/j.rser.2017.01.038).
- 588 [23] C. Sagüés, P. García-Bacaicoa, S. Serrano, Automatic control of biomass gasifiers using fuzzy inference systems,
589 *Bioresour. Technol.* 98 (4) (2007) 845–855. [doi:10.1016/j.biortech.2006.03.004](https://doi.org/10.1016/j.biortech.2006.03.004).
- 590 [24] A. S. Gandhi, T. Kannadasan, R. Suresh, Biomass downdraft gasifier controller using intelligent techniques, in:
591 Y. Yun (Ed.), *Gasification for Practical Applications*, IntechOpen, 2012. [doi:10.5772/48564](https://doi.org/10.5772/48564).
- 592 [25] B. Gøbel, U. Henriksen, T. K. Jensen, B. Qvale, N. Houbak, The development of a computer model for a
593 fixed bed gasifier and its use for optimization and control, *Bioresour. Technol.* 98 (10) (2007) 2043–2052.
594 [doi:10.1016/j.biortech.2006.08.019](https://doi.org/10.1016/j.biortech.2006.08.019).
- 595 [26] N. Striūgas, K. Zakarauskas, A. Džiugys, R. Navakas, R. Paulauskas, An evaluation of performance of automati-
596 cally operated multi-fuel downdraft gasifier for energy production, *Appl. Therm. Eng.* 73 (1) (2014) 1151–1159.
597 [doi:10.1016/j.applthermaleng.2014.09.007](https://doi.org/10.1016/j.applthermaleng.2014.09.007).
- 598 [27] P. V. Daniel, A. S. Gandhi, [Enhanced conventional PID controller for temperature control in woody gasifier using](#)
599 [searching algorithms](#), *International Journal of Innovative Technology and Exploring Engineering (IJITEE)* (4)
600 (2019) 438–442.
601 URL <https://www.ijitee.org/wp-content/uploads/papers/v8i4s/DS2903028419.pdf>
- 602 [28] M. Owen, R. Ripken, [Bioenergy for Sustainable Energy Access in Africa](#), Tech. rep., LTS International Limited,

- 603 the University of Edinburgh and E4tec (2017).
- 604 URL [https://www.erm.com/contentassets/553cd40a6def42b196e32e4d70e149a1/bioenergy-](https://www.erm.com/contentassets/553cd40a6def42b196e32e4d70e149a1/bioenergy-for-sustainable-energy-access-in-africa---a-scoping-study-of-the-opportunities-and-challenges-of-bioenergy-replication-across-sub-saharan-africa-2018.pdf)
- 605 [for-sustainable-energy-access-in-africa---a-scoping-study-of-the-opportunities-and-](https://www.erm.com/contentassets/553cd40a6def42b196e32e4d70e149a1/bioenergy-for-sustainable-energy-access-in-africa---a-scoping-study-of-the-opportunities-and-challenges-of-bioenergy-replication-across-sub-saharan-africa-2018.pdf)
- 606 [challenges-of-bioenergy-replication-across-sub-saharan-africa-2018.pdf](https://www.erm.com/contentassets/553cd40a6def42b196e32e4d70e149a1/bioenergy-for-sustainable-energy-access-in-africa---a-scoping-study-of-the-opportunities-and-challenges-of-bioenergy-replication-across-sub-saharan-africa-2018.pdf)
- 607 [29] V. S. Sikarwar, M. Zhao, P. S. Fennell, N. Shah, E. J. Anthony, Progress in biofuel production from gasification,
- 608 Prog. Energy Combust. Sci. 61 (2017) 189–248. doi:10.1016/j.pecs.2017.04.001.
- 609 [30] M. L. V. Rios, A. M. González, E. E. S. Lora, O. A. A. del Olmo, Reduction of tar generated during biomass
- 610 gasification: A review, Biomass and Bioenergy 108 (2018) 345–370. doi:10.1016/J.BIOMBIOE.2017.12.
- 611 002.
- 612 [31] A. Escámez, R. Aguado, D. Sánchez-Lozano, F. Jurado, D. Vera, An ensemble multi-ANN approach for virtual
- 613 oxygen sensing and air leakage prediction in biomass gasification plants, Renew. Energy 242 (2025) 122376.
- 614 doi:10.1016/j.renene.2025.122376.
- 615 [32] C. Huang, S. Wang, Y. Chu, Y. Chen, X. Chen, L. Liu, H. Zhang, Comprehensive investigations on the explosion
- 616 suppression of biomass fuels: Starch as a representative, Fuel 315 (2022) 123276. doi:10.1016/j.fuel.
- 617 2022.123276.
- 618 [33] G. Liang, H. Dai, H. Yin, Q. Zhao, X. Chen, Inhibition characteristics of coal dust explosion at the gasification
- 619 atmosphere, Advanced Powder Technology 32 (2021). doi:10.1016/j.appt.2021.08.026.
- 620 [34] S. Lin, Z. Liu, J. Qian, X. Li, Comparison on the explosivity of coal dust and of its explosion solid residues to
- 621 assess the severity of re-explosion, Fuel 251 (2019). doi:10.1016/j.fuel.2019.04.080.
- 622 [35] A. Gagliano, F. Nocera, M. Bruno, G. Cardillo, Development of an equilibrium-based model of gasification of
- 623 biomass by Aspen Plus, Energy Procedia 111 (2017) 1010–1019. doi:10.1016/j.egypro.2017.03.264.
- 624 [36] R. Aguado, D. Vera, F. Jurado, G. Beltrán, An integrated gasification plant for electric power generation from
- 625 wet biomass: toward a sustainable production in the olive oil industry, Biomass Conv. Bioref. (2022). doi:
- 626 10.1007/s13399-021-02231-0.
- 627 [37] W. Salah, D. Ishak, K. Hammadi, PWM switching strategy for torque ripple minimization in BLDC motor 62 (3)
- 628 141–146. doi:10.2478/v10187-011-0023-1.
- 629 [38] M. C. Di Piazza, M. Pucci, Techniques for efficiency improvement in pwm motor drives, Electric Power Systems
- 630 Research 136 (2016) 270–280. doi:10.1016/j.epsr.2016.02.031.
- 631 [39] P. P. Divyang, V. Mehta, Design of high accurate universal intelligent temperature transmitter, IJSTE-
- 632 International Journal of Science Technology & Engineering 4 (2018) 162–168.
- 633 [40] T. Witt, R. Mena, E. Cornell, Single chip, 2-wire, 4–20 mA current loop RTD temperature transmitter de-

- 634 sign, IECON Proceedings (Industrial Electronics Conference) (2014) 2380–2383doi:10.1109/IECON.2014.
635 7048837.
- 636 [41] R. Raj, J. V. Tirkey, P. Jena, L. K. Prajapati, Comparative analysis of Gasifier-CI engine performance and emis-
637 sions characteristics using diesel with producer gas derived from coal– briquette–coconut shell–mahua feedstock
638 and its blends, Energy 293 (2024) 130708. doi:10.1016/j.energy.2024.130708.
- 639 [42] M. Tabaa, B. Chouri, S. Saadaoui, K. Alami, Industrial Communication based on Modbus and Node-RED,
640 Procedia Computer Science 130 (2018) 583–588, the 9th International Conference on Ambient Systems, Net-
641 works and Technologies (ANT 2018) / The 8th International Conference on Sustainable Energy Information
642 Technology (SEIT-2018) / Affiliated Workshops. doi:10.1016/j.procs.2018.04.107.
- 643 [43] P. Neumann, Communication in industrial automation—What is going on?, Control Engineering Practice 15 (11)
644 (2007) 1332–1347, special Issue on Manufacturing Plant Control: Challenges and Issues. doi:10.1016/j.
645 conengprac.2006.10.004.